



## Original Research

### Investigation of cochlear hair cells and the perception of ultrasound signals in guinea pigs

Fu-Sen Wang<sup>1</sup>, Guohui Nie<sup>2\*</sup>, Cheng-Cheng Huang<sup>3</sup>, Qian Li<sup>4</sup>, Tiegang Li<sup>5</sup>, Yuee Zou<sup>6</sup>, Shaoyan Zhang<sup>1</sup>, Xinyu Ceng<sup>1</sup>

<sup>1</sup> Department of Otorhinolaryngology, Southern Medical University Affiliated Shenzhen Baoan Hospital, Shenzhen, China

<sup>2</sup> Department of Otorhinolaryngology, the Second People's Hospital of Shenzhen city, Shenzhen, China

<sup>3</sup> Department of Otorhinolaryngology, Wuhan General hospital of PLA, Wuhan, China

<sup>4</sup> Chinese People's Liberation Army 301 Hospital ENT Research Institute, Beijing, China

<sup>5</sup> Molecular Imaging Centre, Institute of Materia Medical, Chinese Academy of Medical Sciences, Beijing, China

<sup>6</sup> Department of electrocardiogram, Southern Medical University Affiliated Shenzhen Baoan Hospital, Shenzhen, China

Correspondence to: [nghui@21cn.com](mailto:nghui@21cn.com)

Received June 13, 2018; Accepted August 14, 2018; Published August 30, 2018

Doi: <http://dx.doi.org/10.14715/cmb/2018.64.11.9>

Copyright: © 2018 by the C.M.B. Association. All rights reserved.

**Abstract:** We established a specific ultrasound frequency-dependent model of cochlear injury using bone conduction ultrasounds in the inner ear of guinea pigs at 50 kHz and 83 kHz, to explore the effects of bone conduction ultrasound in the cochlea. To establish a unilateral cochlear damage model, the unilateral cochlea was destroyed. The control group consisted of 50 kHz and 83 kHz bone conduction ultrasounds in unaltered guinea pigs. In each group, cerebral blood oxygenation level dependent (BOLD) effects were determined by functional magnetic resonance imaging (fMRI). The cochlear outer hair cell motor protein, Prestin, and the microfilament protein, F-Actin, were detected. We found that bone conduction ultrasound irradiation at 50 kHz and 83 kHz on the guinea pig inner ear for six hours leads to hair cell damage. Furthermore, low frequency bone conduction ultrasound induces major damage to outer hair cells, while high frequency ultrasound damages both internal and external hair cells. fMRI analysis of cerebral BOLD effects revealed an affected cerebral cortex region of interest (ROI) of 4 and 2, respectively, for the normal control group at 50 kHz or 83 kHz, and 2 for the 83 kHz bone conduction ultrasound cochlear injury group, while 50 kHz bone conduction ultrasound failed to induce the cortical ROI within injury model. Results reveal that the spatial location of guinea pig cochlear hair cells determines coding function for lower ultrasound frequencies, and high frequency bone conduction ultrasound may affect the cochlear spiral ganglion or cranial nerve nucleus in bone conduction ultrasound periphery perception.

**Key words:** Cochlear hair cells; Ultrasound signals; Guinea pigs; Cochlear damage model.

## Introduction

Ultrasonic transmission has potential applications ranging from hearing rehabilitation to underwater communication (1-7). However, the auditory peripheral sensations, conduction pathways, and cortical perception mechanisms that underlie ultrasonic transmission remain poorly understood. Various groups have studied ultrasound terminal sensory mechanisms using bone conduction ultrasound at 98.8 kHz and 143.5 kHz, to induce the near-field potential of guinea pig cochlea. These studies have shown that ultrasound terminal receptors reside in the cochlea, and communicate with inner hair cells in a specific manner (8).

Lenhardt et al. was the first group to describe the use of bone conduction ultrasound hearing aids for severe sensorineural hearing loss in patients with normal balloon function. Greater rates of speech recognition have been observed in patients with ultrasonic hearing aids than in the control group. This suggests that ultrasound peripheral receptors reside in the balloon (9). Other investigations of verbal recognition rate in patients using masked ultrasound language modulation, have shown that ultrasonic language is different from non-adjusted ultrasound language in patients with severe deafness. These results revealed that direct stimulation by ultrasound signals plays an important role in perception in

patients with severe deafness (10). Wang et al studied the impact of ultrasound signals on cochlear hair cells in Guinea pigs. In this study, authors valued the histologic and histochemical (succinate dehydrogenase, SDH) changes in cochleas of guinea pigs after non-focused ultrasound (NFU) irradiation. The data show that a certain dosage of NFU irradiation at various frequencies could lead to metabolic changes in the basilar membrane and stria vascularis at different areas of cochlea. Moreover, these changes were found to be reversible or partially reversible. These changes also suggest that the cochlear hair cells located at different areas might be related to ultrasonic perception (11).

It has recently been discovered that mice can emit ultrasound and perceive ultrasonic signals up to 100 kHz (10). However, this is significantly greater than the range of human ultrasonic signal perception (10). On the other hand, human and guinea pig cochlea have significant structural and physiological similarities. Therefore, we selected guinea pigs as our research model. We exposed the cochlea of guinea pigs to specific doses of low and high frequency bone conduction ultrasound to establish a frequency-dependent cochlear hair cell-specific injury model. We quantified cerebral blood oxygenation level dependent (BOLD) effects within the cortex region of interest (ROI). Click and bone conduction ultrasound signals were induced in the normal guinea pigs, the ul-

trasound cochlear injury model, and the unilateral cochlear damage model. Cerebral BOLD effects on the ROI were determined by functional magnetic resonance imaging. We performed immunofluorescence analysis of the cochlear outer hair cell motor protein, Prestin, and the microfilament protein, F-Actin, to explore the localisation of ultrasound peripheral receptors and the potential coding mechanisms of ultrasonic signals within the cochlea.

## Materials and Methods

### Laboratory animals and animal groups

Forty healthy white guinea pigs were selected that were 3 months old, weighed 250–300 g, and expressed ear reflex sensitivity. The animals were randomly divided into the normal control group, one of two ultrasound cochlear injury groups, or a unilateral cochlear injury group. Each group contained 10 animals (20 ears).

### Preparation of a guinea pig cochlear ultrasound injury model

Guinea pig ear hair was shaved at a diameter of 2 cm, after which an intraperitoneal injection of 1% pentobarbital sodium was performed on anaesthetised animals. A thermostat was fixed to the operating table, and tracheal intubation was performed with an animal ventilator (MIDMARK). Respiratory rate was maintained at 40–60 breaths per minute, and blood oxygen saturation was maintained at greater than 90%. The left ear mastoid area was coated with liquid paraffin, and an ultrasonic probe (3 mm diameter) was used to fix the face-fit bone surface. Cochlea were irradiated with 50 kHz or 83 kHz ultrasonic waves at 100 db for 6 h.

### Preparation of a unilateral cochlear damage model

First, an intraperitoneal injection of 1% pentobarbital sodium was performed under anaesthesia, with a thermostat fixed to the operating table. The organ was cut for intubation with the animal ventilator. Respiratory rate was maintained at 40–60 breaths per minute, and blood oxygen saturation was maintained at greater than 90%. A surgical microscope was used to expose and damage the bubble.

### fMRI detection of cerebral BOLD effects in injury models vs. control groups, during the induction of bone conduction ultrasound

Respiratory cells were measured by isoflurane gas inhalation anaesthesia. Respiratory rate was maintained at 40–60 breaths per minute, and oxygen saturation was maintained at greater than 90%. Magnetic resonance scanning was performed using a Bruker 7.0T Superconducting Magnetic Resonance Imaging System. A single channel, small animal head, high resolution phased array coil was used. After positioning the scan, functional images were acquired during 50 kHz and 83 kHz bone conduction ultrasounds for the unaltered control group, 50 kHz bone conduction ultrasound for one cochlear injury group, and 83 kHz bone conduction ultrasound for the other cochlear injury group. To examine the cerebral cortex ROI, within the right ear, a short sound (click) was induced, while 83 kHz bone conduction ultrasound was induced within the left ear to stimulate cochlear in-

jury. Induction parameters: TR2000, TE20; repetitions: 600; scan time: 20 minutes; 0–5 minutes of no sound, 5–10 minutes of sound stimulation, 10–15 minutes of no sound stimulation, and 15–20 minutes of sound stimulation.

### fMRI analysis procedure

Data pre-processing was performed in SPM12. The first 5 five scans in resting conditions were discarded to reduce the influence of T1 on contrast of the image series.

Each fMRI image series was realigned to reduce motion artefacts by six-parameter rigid spatial transformation and six motion parameters were obtained which were used in other regressors in the general linear model.

Co-registration of the structural T1-weighted image with the mean fMRI image was performed, by normalised mutual information with a separation of  $2 \times 1$  mm.

Each subject's structural image was registered onto a group reference structural image, by normalised cross-correlation, with a separation of  $4 \text{ mm} \times 2 \text{ mm}$ . The same transformation matrix was applied onto each subject's fMRI image series, and re-sliced as in the group reference.

Spatial smoothing of all fMRI images was performed in  $1 \times 1 \times 1$  mm (approximately  $2 \times$  resolution).

### Pre-processing of results

During realignment steps, subjects were reported that displayed a large translation or rotation of the head ( $>3$  mm or  $>3$  degree); subjects displaying such head artefacts were discarded.

Forty functional MRI image series remained in the analysis pipeline, and head movement artefacts were observed in 6 images.

### Model estimation in SPM12

The adopted model was the general linear model of nine regressors and one constant.

Regressor of interest: Activation of the brain region upon stimulation over time, which pertains to the left-most column of the design matrix of the model.

Regressors not of interest: Six head motion parameters over time, the average intensity of the ROI of white matter over time, and the average intensity of the ROI water content over time.

Designed matrix of the model.

ROI filtering masks of both the white matter (red) and cerebrospinal fluid (green) were applied.

A T-contrast of  $[1 \ 0 \ 0 \ 0 \ 0 \ 0 \ 0 \ 0 \ 0]$  was used to visualise the directional activation of the region upon auditory stimuli.

Significant criteria:  $p(\text{FWE-corrected}) < 0.05$  or  $p(\text{uncorrected}) < 0.001$ , were used in the former, to help to eliminate the significant noise cluster.

Significant clusters that lie on the region of interest within the fMRI image boundary were reported.

Reference region of interest for auditory pathway resolution (Voxel size):  $0.549 \times 0.549 \times 0.5$  mm.

The region of interest was based on a previous study which revealed activation of the auditory pathway region of an fMRI, upon listening to a pure tone sound. These regions are taken, as reference, to locate the ro-

dent brain auditory functional area.

A mask was added to the general linear model, to restrict the ROI to within the brain region.

### Immunofluorescent labelling of Prestin and F-actin detection with Phalloidin via confocal microscopy

After the cerebral BLOD effect was tested by fMRI, the guinea pigs were sacrificed. The auditory bubble was removed and fixed in 4% paraformaldehyde. The basement membrane was removed by anatomical dissection after 8 hours of immobilisation and stained for the cochlea hair cell motor protein, Prestin, via immunofluorescence labelling, in addition to phalloidin staining of F-actin. Immunofluorescent images were acquired using a confocal microscope.

### Immunofluorescence detection reagents and equipment

Primary anti-Prestin 1: Primary (rabbit anti-Prestin 1:200, Santa Cruz, SC-30163), secondary antibody (Alexa Fluor 568 conjugated goat anti-rabbit IgG, 1:1000, Molecular probe, A-11011), F-actin microfilm fluorescent staining (Alexa Fluor 488 Phalloidin, 1:200, Molecular probe, A12379), and confocal microscope (Zeiss LSM800).

## Results

### Guinea pig cerebral cortex BLOD effect, fMRI test of bone conduction ultrasound-induced injury models vs. control group

The 50 KHz bone conduction ultrasound-induced control group BLOD effect of fMRI was induced in the cerebral cortex region of interest (ROI) in four (Figures 1 and 2) animals, and two normal guinea pigs were successfully induced in the cortical ROI with 83 KHz bone conduction ultrasound. Two 83 KHz bone conduction ultrasound cochlear injury model guinea pigs were successfully induced within the cerebral cortex ROI (Figures 3 and 4), while the 50 KHz ultrasound cochlear injury model failed to induce an effect.

The left cochlear removed group was successfully induced, as shown by a cortical BLOD effect within the ROI of two guinea pigs. A click induced the ROI for the control area, followed by ROI induction with bone conduction ultrasound (Figure 5).

### Prestin and F-actin detection in control vs. cochlear ultrasound injury groups

In the 50 kHz bone conduction ultrasound cochlear injury group, from the beginning of the basement membrane,  $800 \pm 10 \mu\text{m}$  to  $840 \pm 5 \mu\text{m}$ , Prestin fluorescence was significantly attenuated compared with the corresponding control group. Furthermore, fluorescent signal corresponding to F-actin showed no significant change (Figures 6 and 7). In the cochlear injury group, fluorescent F-actin staining of outer hair cells was significantly lower than that of the control group, while no significant change was observed in the inner hair cells (Figure 8).

In the 83 kHz bone conduction ultrasound cochlear injury group, from the bottom of the basement membrane,  $40 \pm 10 \mu\text{m}$  to  $75 \pm 5 \mu\text{m}$ , F-actin fluorescent staining of hair cells was significantly attenuated relative to the corresponding control group (Figure 9). In

the 83 kHz bone conduction ultrasound cochlear injury group, Prestin and F-actin fluorescent signals were lower than those of the control group in the contralateral ear (non-ultrasonic ear) cochlear basement membrane, which corresponds to  $35 \pm 5 \mu\text{m}$  from the cochlear hair cells (Figure 10). However, relative to the same group of bone conduction ultrasound irradiated hair cells, Prestin

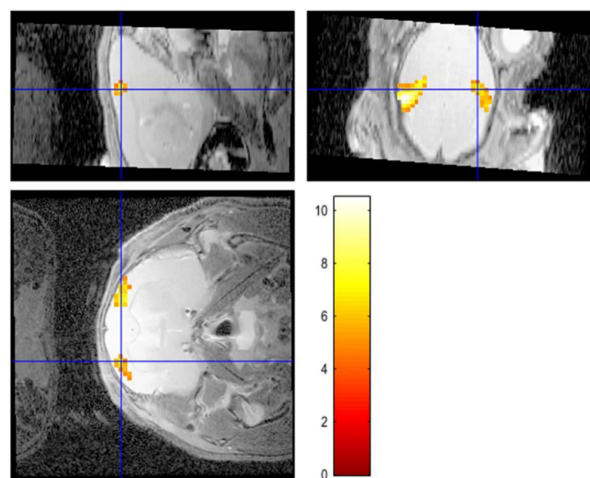


**Figure 1.** Apoptosis of 50 kHz bone-guided ultrasound cochlear injury cortical BLOD ROI (57voxels, four in ten Guinea pigs).

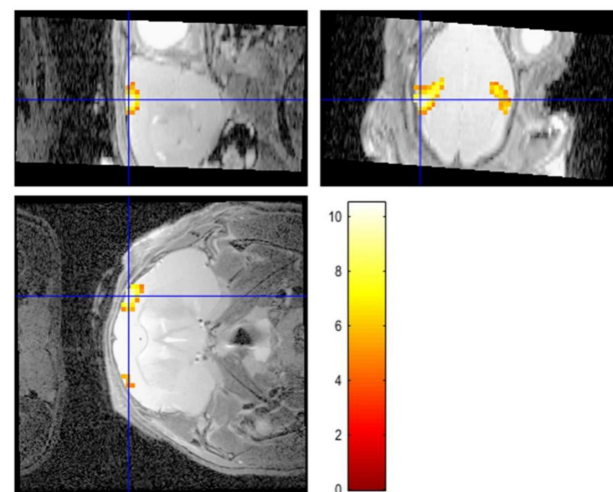


**Figure 2.** Apoptosis of 50 kHz bone-guided ultrasound cochlear injury cortical BLOD ROI (111 voxels, four in ten Guinea pigs).

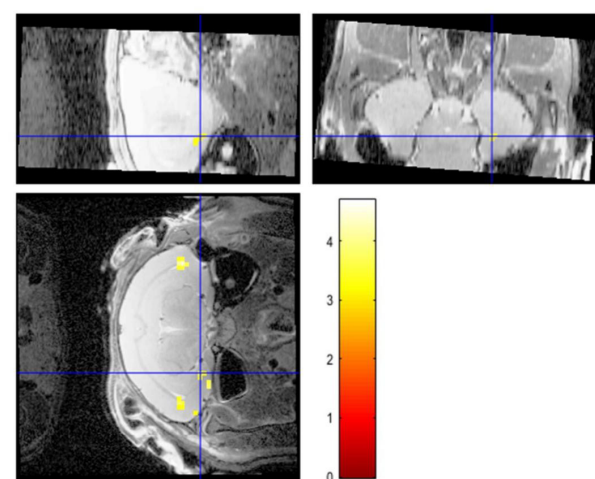


**Figure 3.** 83 kHz bone conduction induced by ultrasound in the normal guinea pig group cortex BLOD ROI (8 voxels, two in ten Guinea pigs).

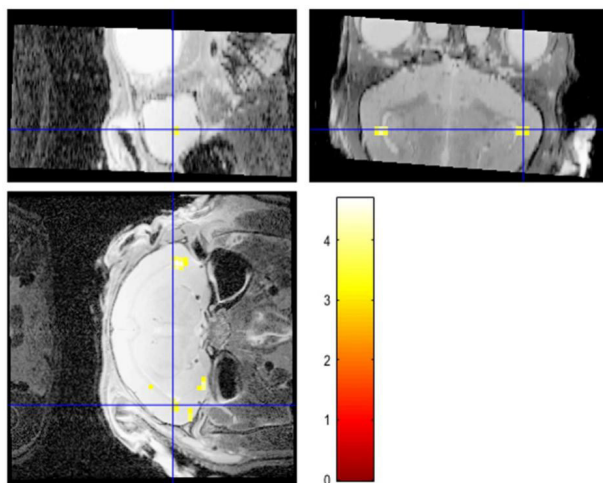


**Figure 4.** 83 kHz bone conduction induced by ultrasound in the 83 kHz bone conduction ultrasound cochlear injury group cortex BLOD ROI (10 voxels, two in ten Guinea pigs).

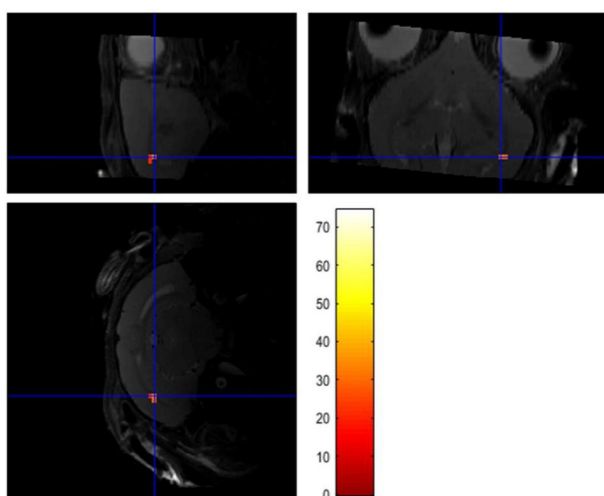


**Figure 5.** Localisation of BLOD in the cortex of the left cochlea removed group induced by bone-guided ultrasound and normal guinea pig cortex BLOD active area (control area) by right ear click ventilation (two guinea pigs).

and F-actin fluorescent signals were strong (Figure 9).

## Discussion

It has been well established that humans can feel bone conduction ultrasound, and bone-conducting hearing aids have been developed to improve voice recognition for patients with severe deafness (12). Currently, the success rate of ultrasonic speech recognition remains low, and the interplay between peripheral ultrasound sensation and centralised perception mechanisms remains unclear.

Ultrasound cochlear electrograms of guinea pigs receiving ultrasonic bone conduction channels at 98.8 kHz and 143.5 kHz have revealed that ultrasound terminal receptors are located within the cochlea, and ultrasound signals are detected by inner hair cells. Furthermore, studies on the generation of bone conduction ultrasound hearing aids, have shown a 40% ultrasound language recognition rate in patients with severe sensorineural hearing loss and normal balloon function, leading to the hypothesis that ultrasound peripheral receptors are in the balloon.

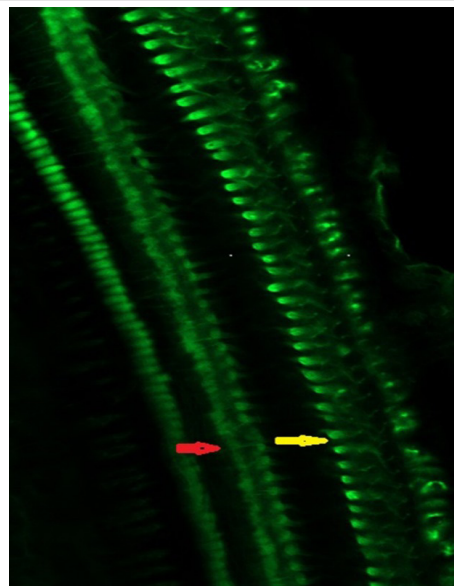


**Figure 6.** Normal guinea pig basement membrane initial segment hair cell microfilament protein (F-actin), with phalloidin staining (green), using laser confocal detection,  $\times 400$  times (Red arrow for the inner hair cells, yellow arrow point to the outer hair cells, ten guinea pigs).

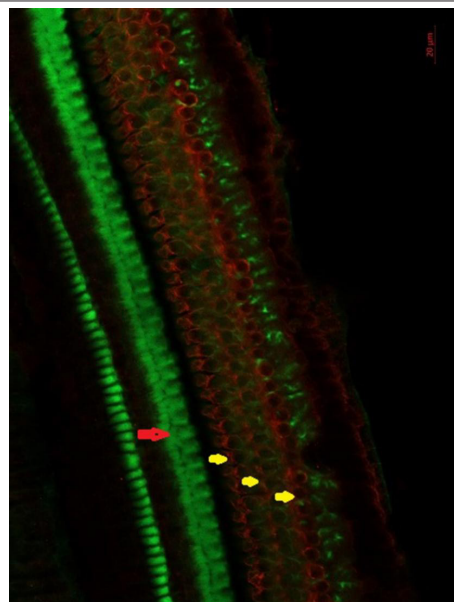


**Figure 7.** The 50 kHz bone conduction ultrasound cochlear injury model group from the basement membrane at the beginning of the segment, from  $800 \pm 10 \mu\text{m}$  to  $840 \pm 5 \mu\text{m}$  range of hair cell motor protein (Prestin) immunofluorescence (red) + microfilament protein (F-actin) phalloidin staining (green) laser confocal detection, outer hair cell damage, inner hair cells, and compared with the normal group, there was no significant change (Red arrow for the inner hair cells, yellow arrow point to the outer hair cells, ten guinea pigs),  $\times 400$  times.

In addition, analysis of the conduction of ultrasonic signals by human bone has suggested that the peripheral organs that detect ultrasound waves are located in the cochlea (13). Some scholars also believe that the bone conduction of ultrasound may directly stimulate spiral ganglion and the brain stem, both of which are expected to play a role in the detection of ultrasound (14). Experiments using an ultrasound Doppler have shown that ultrasound is detected, in humans, through vibration of the human cochlea basement membrane and the round window bones (15).

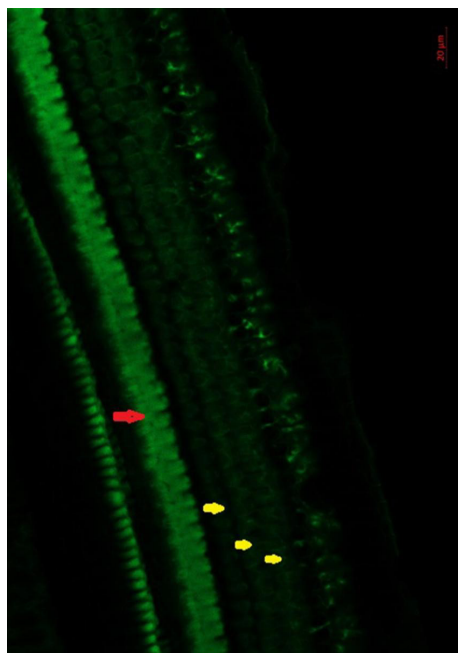


**Figure 8.** The 50 kHz bone conduction ultrasound cochlear injury model group from the basement membrane at the beginning, from  $800 \pm 10 \mu\text{m}$  to  $840 \pm 5 \mu\text{m}$  range of microfilament protein (F-actin) phalloidin staining (green) laser confocal detection, outer hair cell damage, inner hair cells, and compared with the normal group, there was no significant change (Red arrow for the inner hair cells, yellow arrow point to the outer hair cells, ten guinea pigs),  $\times 400$  times.

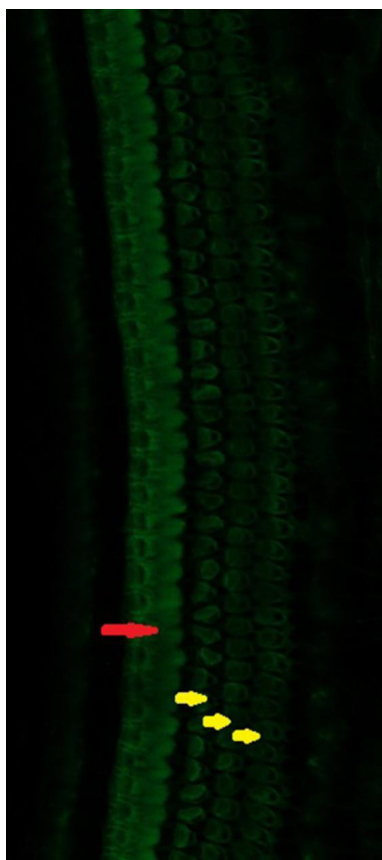


**Figure 9.** The 83 kHz bone conduction ultrasound cochlea injury model group from the basement membrane at the beginning of the segment, from  $40 \pm 10 \mu\text{m}$  to  $75 \pm 5 \mu\text{m}$  range cochlear hair cells microfilament protein (F-actin), phalloidin staining (green), laser confocal detection, and inner hair cells, outer hair cell fluorescence were weakened (Red arrow for the inner hair cells, yellow arrow point to the outer hair cells, ten guinea pigs),  $\times 400$  times.

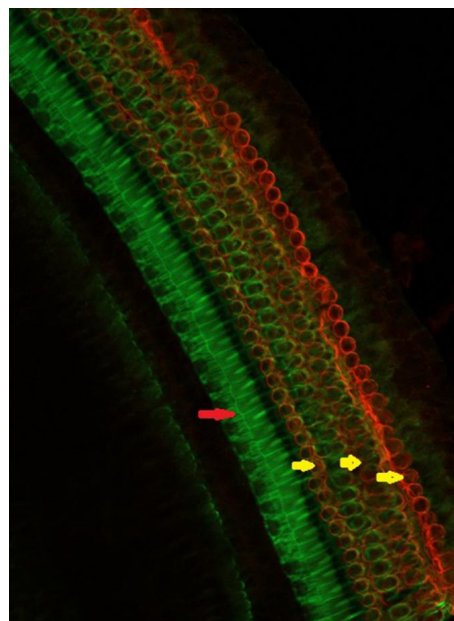


**Figure 10.** The 83 kHz bone conduction ultrasound cochlear injury model group of the contralateral ear (non-direct ear) from the beginning of the basement membrane at the beginning from  $40 \pm 10 \mu\text{m}$  to  $75 \pm 5 \mu\text{m}$  range of hair cell motor protein (Prestin) immunofluorescence (red) + microfilament protein (F-actin), phalloidin staining (green), laser confocal detection, and inner hair cells, outer hair cell injury (Red arrow for the inner hair cells, yellow arrow point to the outer hair cells, ten guinea pigs),  $\times 400$  times.

Masked ultrasound language modulation tests have been employed by various research groups to test verbal recognition rates. Studies using this test have shown that ultrasound language in patients with severe deafness is processed differently from non-adjusted ultrasound language signals, while normal sounds are perceived similarly. This suggests that ultrasonic stimulation plays an important sensory role in patients with severe deafness (10). Ultrasonic signals can also evoke cortical potentials in rats and alter behavioural responses in mice (16).

Mice emit ultrasonic signals up to 70 kHz and sense signals up to 100 kHz. As human and guinea pig cochlea have substantial structural and physiological similarities, we selected guinea pigs as our research model for this study. To establish an ultrasound cochlear injury model, we irradiated guinea pigs for six hours with different frequencies of bone conduction ultrasonic signals. Different frequencies of bone conduction ultrasound have been observed to differ in their effects on succinate dehydrogenase activity within hair cells (11).

In our experiment, we used low frequency bone conduction ultrasound at 50 kHz and high-frequency bone conduction ultrasound at 83 kHz to irradiate guinea pig cochlea for six hours, and performed an immunofluorescence analysis of Prestin, and Phalloidin staining of F-actin. We discovered that low frequency ultrasound damages specific regions of the outer hair cells. Furthermore, high frequency bone conduction ultrasound at 83 kHz causes internal and external hair cell damage.

We used 50 kHz and 83 kHz bone conduction ultrasound to induce injury in normal guinea pigs, and examined the cerebral BLOD effect within a specific ROI. There were 4 (50 kHz) and 2 (83 kHz) bone conduction ultrasounds in 10 normal guinea pigs that were found to induce the cerebral cortex ROI, while 10 cases of the

50 kHz bone conduction ultrasound in the injury model failed to induce the cerebral cortex ROI. Only 2 cases of 83 kHz bone conduction ultrasound in the injury model induced the cerebral cortex ROI. The different frequencies of bone conduction ultrasound signal-induced cerebral cortex ROI did not completely overlap, which indicates that the sensation of lower frequency ultrasound requires the participation of peripheral cochlear hair cells, while higher frequencies require additional receptors.

In our experiment, low frequencies of bone conduction ultrasound induced cochlear resection of the lateral cerebral cortex ROI, which further demonstrates that low frequency bone conduction ultrasound signals are sensed by peripheral cochlear hair cells. Bone conduction ultrasound induces a low specific cerebral cortex ROI ratio, which may be related to the lack of ideal acoustic shielding and the induced parameters of bone conduction ultrasound signals. Such parameters require further improvement. In addition, the standardisation of animal anaesthesia needs to be addressed.

In this study, we found that low and high frequency bone conduction ultrasound irradiation of guinea pig cochlea causes a variety of injuries within the hair cell region. Low frequency ultrasound irradiation of guinea pig cochlea mainly damages the outer hair cells, while high frequency bone conduction ultrasound injures both inner and outer hair cells. Hair cell space is involved in peripheral code recognition of low frequency ultrasonic signals. High frequency bone conduction ultrasound stimulates spiral ganglion or the brain stem-related nucleus, which directly experience the ultrasound signal. Different areas in the guinea pig cortex recognise acoustic signals of various frequencies, and the size of each recognition area is unique.

### Acknowledgments

Professor Wang Ji Bao from the Department of Otolaryngology, Wuhan Union Medical College Hospital guided me in the field of ultrasound auditory research. Professor Wang Defeng and Professor Shi Lin from Prince of Wales Hospital Imaging Centre, Hong Kong aided in the fMRI data analysis.

The study was supported by Science and Technology Program of the Guangdong Science and Technology Department (2014A020212616), Science and Technology Program of the Shenzhen Science and Technology Innovation Commission (JCYJ20150402152005639).

### Interest conflict

There is no conflict of interest to be declared by the au-

thor.

### References

1. Tsukano H, Horie M, Bo T, Uchimura A, Hishida R, Kudoh M, et al. Delineation of a frequency-organized region isolated from the mouse primary auditory cortex. *J Neurophysiol* 2015; 113: 2900-2920.
2. Du Y, Ping J, Li N, Wu X, Li L, Galbraith G. Ultrasonic evoked responses in rat cochlear nucleus. *Brain Res* 2007; 1172: 40-47.
3. Portfors CV, Perkel DJ. The role of ultrasonic vocalisations in mouse communication. *Curr Opin Neurobiol* 2014; 28: 115-120.
4. Ferhat AT, Torquet N, Le Sourd AM, Chaumont F, Olivo-Marin JC, Faure P, et al. Recording mouse ultrasonic vocalisations to evaluate social communication. *J Vis Exp* 2016; 112: 53871.
5. Schwarting RK, Wöhr M. On the relationships between ultrasonic calling and anxiety-related behaviour in rats. *Braz J Med Biol Res* 2012; 45: 337-348.
6. Garcia-Lazaro JA, Shepard KN, Miranda JA, Liu RC, Lesica NA. An overrepresentation of high frequencies in the mouse inferior colliculus supports the processing of ultrasonic vocalisations. *PLoS One* 2015; 10: 133251.
7. Lau C, Zhang JW, Cheng JS, Zhou IY, Cheung MM, Wu EX. Non-invasive fMRI investigation of inter-aural level difference processing in the rat auditory subcortex. *PLoS One* 2013; 8: 70706.
8. Ohshima K, Kusakari J, Kawamoto K. Ultrasonic electrocochleography in guinea pig. *Hear Res* 1985; 17: 143-151.
9. Lenhardt ML, Skellett R, Wang P, Clarke AM. Human ultrasonic speech perception. *Sci* 1991; 253: 82-85.
10. Nishimura T, Okayasu T, Saito O, Shimokura R, Yamashita A, Yamanaka T, et al. An examination of the effects of broadband air-conduction masker on the speech intelligibility of speech-modulated bone-conduction ultrasound. *Hear Res* 2014; 317: 41-49.
11. Matsumoto J, Nishimaru H, Takamura Y, Urakawa S, Ono T, Nishijo H. Amygdalar auditory neurons contribute to self-other distinction during ultrasonic social vocalisation in rats. *Front Neurosci* 2016; 10: 399.
12. Nishimura T, Okayasu T, Uratani Y, Fukuda F, Saito O, Hosoi H. Peripheral perception mechanism of ultrasonic hearing. *Hear Res* 2011; 277: 176-183.
13. Okayasu T, Nishimura T, Yamashita A, Saito O, Fukuda F, Yanai S, et al. Human ultrasonic hearing is induced by a direct ultrasonic stimulation of the cochlea. *Neurosci Lett* 2013; 539: 71-76.
14. Torbatian Z, Garland P, Adamson R, Savage J, Bance M, Brown J. Listening to the cochlea with high-frequency ultrasound. *Ultrasound Med Biol* 2012; 38: 2208-2217.
15. Stiebler I. A distinct ultrasound-processing area in the auditory cortex of the mouse. *Natwiss* 1987; 74: 96-97.
16. Wang F, Wang J, Gong S. A study of the histologic and enzyme histochemical changes in the cochlea of guinea pigs after non-focused ultrasound irradiation. *Cell Biochem Biophys* 2013; 66: 409-415.